50 and 10 °K. It is believed that the low-temperature hopping conduction observed in our In-doped CdS samples is taking place at this unknown donor state because the thermal energy in this temperature range is much smaller than E_{D2}. Optical-transmission experiments revealed another defect level at 0.175 eV below the band edge. The scattering of electrons is independent of the types of impurities for $T > 200$ °K and is mainly due to the longitudinal optical-mode scattering. Impurity-hopping conduction was observed for In-doped CdS for $T < 20$ °K. This was not observed for the case of Cu-doped CdS with the same amount of impurity concentration.

†Research supported in part by the Graduate School of the University of Florida through a 1970 Summer Research Support Grant and in part by ARPA and monitored by AFCRL under Contract No. F19628-68-C-0058.

[1]F. A. Kroger, H. J. Vink, and J. Volger, Philips Res. Rept. 10, 39 (1955).

[2]H. Miyazawa, H. Maeda, and H. Tomishima, J. Phys. Soc. Japan 14, 41 (1959).

[3]S. S. Devlin, L. R. Shiozawa, and J. M. Jost, Final Report, Contract No. ARL-65-98, Aerospace Research Laboratories, Wright-Patterson Air Force Base, Ohio, 1965 (unpublished).

[4]H. Fujita, K. Kobayashi, T. Sawai, and K. Shiga, J. Phys. Soc. Japan 20, 109 (1965).

[5]A. G. Redfield, Phys. Rev. 94, 526 (1954).

[6]K. Morikawa, J. Phys. Soc. Japan 20, 1728 (1965).

[7]H. H. Woodbury and M. Aven, in *Proceedings of the Seventh International Conference on the Physics of Semiconductors* (Academic, New York, 1964), p. 179.

[8]G. W. Bradberry and W. E. Spear, Brit. J. Appl. Phys. 15, 1127 (1964).

[9]V. Buget and G. T. Wright, Brit. J. Appl. Phys. 16, 1457 (1965).

[10]W. W. Piper and R. E. Halsted, in *Proceedings of the International Conference on Semiconductor Physics, Prague*, 1960 (Academic, New York, 1961), p. 1046.

[11]M. Itakura and H. Toyoda, J. Phys. Soc. Japan 18, 150 (1963).

[12]T. H. Geballe, *Semiconductors*, edited by N. B. Hannay (Reinhold, New York, 1959), p. 313.

[13]$N_A = 1 \times 10^{17}$ cm^{-3} is chosen so that consistent results in the curve fit of Fig. 2 can be obtained for $20 < T < 300$ °K.

[14]See, for example, R. H. Bube, *Photoconductivity of Solids* (Wiley, New York, 1960), p. 160.

[15]A. F. Gibson and R. E. Burgess, *Progress in Semiconductors* (Wiley, New York, 1964), Vol. 8, p. 80.

[16]K. Nassau, C. H. Henry, and J. W. Shiever, Proceedings of the 10th International Conference on Semiconductor Physics, 1970 (unpublished), p. 629.

PHYSICAL REVIEW B VOLUME 3, NUMBER 10 15 MAY 1971

Light Scattering from Acoustic Plasma Waves and Single-Particle Excitations in Semiconductor Magnetoplasmas*

F. A. Blum and R. W. Davies

Lincoln Laboratory, Massachusetts Institute of Technology, Lexington, Massachusetts 02173

(Received 10 December 1970)

A theoretical discussion of inelastic light scattering from acoustic plasma waves and single-particle excitations in a one-component spherical-band semiconductor plasma in a magnetic field is given. A phenomenological relaxation time is used to treat collisional effects. Detailed scattering spectra are computed as a function of magnetic field using physical parameters appropriate for infrared experiments with conduction electrons in indium antimonide. It is shown that screening effects predicted by a simple effective-mass theory are grossly different from those predicted by a more realistic theory which properly treats virtual interband transitions. The general results indicate that the acoustic-plasma-wave damping in high magnetic fields is sufficiently small and the cross section is sufficiently large to yield an unambiguous spectral identification of this wave with currently available experimental apparatus.

I. INTRODUCTION

In the absence of a dc magnetic field $\vec{B}_0$, the cross section for inelastic light scattering from a single-component plasma in a semiconductor exhibits[1] (for long wavelengths) (a) broad quasi-elastic scattering of single particles in the frequency range $0 \lesssim \omega \lesssim q v_c$, where v_c is a characteristic particle speed and q is the scattering wave-vector magnitude, and (b) plasma-wave scattering near $\omega = \omega_p$, the free-carrier plasma frequency.[2] Both of these scattering processes have been observed[3-8] and theoretically discussed.[4,9-14] If a magnetic field is applied to the plasma, the scattering spectra peaks occur in similar frequency bands. However, if one considers a strong field applied to low-temperature (degenerate) carriers, so that Landau orbital quantization is important,

the quasi-elastic scattering is drastically altered.[15,16] The electrons on each occupied Landau level effectively become a one-dimensional electron gas, and the single-particle scattering spectrum splits into a series of separated peaks. Furthermore, for long relaxation times, the quasi-elastic scattering will have additional peaks[15,16] due to the excitation of longitudinal acoustic (LA) plasma waves[17-19] at frequencies between the single-particle peaks. Neither of these features of magnetoplasma quasielastic light scattering has been observed.

Wolff[16] has given some specific theoretical discussion of this magnetoplasma scattering in addition to the general discussion given by Blum.[15] He discusses the coupling via spin-density fluctuations to the highest-lying acoustic plasma mode in III-V compound semiconductors. He treats the case in which only the two lowest Landau levels are occupied, and concludes that the acoustic plasma-wave scattering should be dominant over the single-particle scattering. Because of the relatively short relaxation times τ in real semiconductors and the multiplicity of scattering resonances in the quasi-elastic regime, the inclusion of relaxation effects is vital to the interpretation and physical understanding of observed scattering spectra. For very short τ and/or weak magnetic fields the multiple peaks may strongly overlap, yielding a broad smooth scattering spectrum similar to that found for zero magnetic field and dominated by single-particle excitations.

This paper gives a theoretical discussion of magnetoplasma quasi-elastic light scattering for spherical-band semiconductors. Particular attention is given to the coupling through both charge-density and spin-density fluctuations. Detailed scattering spectra are computed as a function of B_0 for realistic physical parameters (including τ) appropriate for infrared experiments with InSb. The calculations of this paper have two primary motivations. First, the subject at hand is a natural extension of zero-field light-scattering work and the chances of experimental observation appear good.[16] The study given here can serve as a valuable guide in performing experiments. Second, whereas the notion of LA plasma waves in solid-state plasmas is well established theoretically, none of the various possible acoustic plasma modes[17-21] has been observed by any technique. Waves included in this important class of plasma waves in solids also occur ($B_0=0$)[17,20,21] in two-component (electrons and holes) and single-component multivalley plasmas in semiconductors and semimetals. They generally involve a weak density perturbation which is not easily coupled to. Light scattering may be the best way to overcome[9,16] this difficulty, and the acoustic plasma waves described here may be the first of this class to be observed.

Section II of this paper discusses the application to the quasi-elastic regime of a general light-scattering cross section which was derived previously.[15,22] In Sec. III we specialize the results of Sec. II to an effective-mass approximation. The light couples to the plasma only through charge-density fluctuations. It is found that for realistic physical parameters the quasi-elastic scattering is rather small, and tends to be washed out and lost in the wings of the plasmon scattering. Some spectra computed with long relaxation times are used to illustrate the basic features of the scattering. Specific discussion of a realistic treatment for degenerate conduction electrons in InSb is given in Sec. IV. Virtual interband transitions are properly accounted for and lead to additional coupling via spin-density fluctuations. Detailed spectra are calculated with magnetic field as a parameter, showing the complex interplay of the various terms in determining the physical nature of the observed spectra. The scattering which involves spin-density fluctuations is not lost in the plasmon wing. For weak fields the scattering is a broad hump resembling the zero-field spectra, and is largely composed of single-electron excitations. For strong fields (particularly for two levels occupied) the spectra develop strong narrow peaks which result from acoustic-plasma-wave excitation. When the field is increased to the point that there is only one level occupied, there are no acoustic-plasma-wave excitations. The scattering reverts to single-electron excitations and is dramatically screened to essentially zero (relative to lower field spectra) over the quasi-elastic regime. This strong screening results from the approximation of the interband matrix elements and is shown not to occur in general. The results of Sec. IV indicate that the acoustic-plasma-wave damping in high fields is sufficiently small and the cross section is sufficiently large to yield unambiguous results with currently available experimental apparatus. Finally, it is shown that in strong magnetic fields the spin-density driving term couples to the optical plasma waves, leading to depolarized plasmon scattering.

II. CROSS SECTION

We have previously included[22] phenomenological damping (orbital and spin) in a calculation of the cross section for inelastic light scattering from semiconductor plasmas in a dc magnetic field. We use this result[22] as a basis of the calculations of this paper. The original cross-section calculation[15] was based on an approach given by Hamilton and McWhorter,[13] and neglected electro-optic and magneto-optic scattering mechanisms. Coulomb inter-

actions were treated in the random phase approximation. The neglect of electro-optic effects should be particularly appropriate for infrared experiments with small-gap semiconductors.[7] It is this class of experiments at which the present discussion is aimed.

The general differential cross section for the scattering of a photon from the state $(\omega_I, \vec{k}_I, \vec{\epsilon}_I)$ to the state $(\omega_F, \vec{k}_F, \vec{\epsilon}_F)$ is given by Eq. (49) of Ref. 22. We can ignore spin relaxation [set $(1/\tau_s)=0$], since the excitations that we consider involve momentum perturbations (with no spin-flips) and, for the situations we consider, spin relaxation times are very long compared to the orbital relaxation times. For the III-V semiconductors this means that we restrict our attention to conduction-band excitations (as opposed to excitations involving valence-band states which are strongly spin-orbit mixed).

We treat the conduction-band states in an effective-mass and effective g-factor approximation and denote the corresponding eigenstates of the one-electron Hamiltonian H_0 by $|i\rangle|\sigma\rangle = |n, k_y, k_z\rangle|\sigma\rangle$ where i represents the orbital quantum numbers and σ the spin quantum number. The energy eigenvalues of H_0 are given by

$$E(k_z, n, \sigma) = \hbar^2 k_z^2/2m^* + \hbar\omega_c\,(n+\tfrac{1}{2}) + \sigma\tfrac{1}{2}\hbar\omega_s\,,$$

where $\hbar\omega_s = g^*\mu_B B_0$ is the spin-flip energy and $\hbar\omega_c = \hbar eB_0/m^*c$ is the cyclotron energy. The first problem one faces in evaluating the cross section is the calculation of the "driving-term" matrix element[15]

$$\gamma_{\alpha\beta} \approx \frac{e^2}{mc^2}\left[\langle\alpha|e^{i\vec{q}\cdot\vec{r}}|\beta\rangle\,\vec{\epsilon}_I\cdot\vec{\epsilon}_F + \frac{1}{m}\sum_{\beta'}\left(\frac{\langle\alpha|\vec{\epsilon}_F\cdot\vec{p}\,e^{-i\vec{k}_F\cdot\vec{r}}|\beta'\rangle\langle\beta'|\vec{\epsilon}_I\cdot\vec{p}\,e^{i\vec{k}_I\cdot\vec{r}}|\beta\rangle}{E_\beta - E_{\beta'} + \hbar\omega_I} + \frac{\langle\alpha|\vec{\epsilon}_I\cdot\vec{p}\,e^{i\vec{k}_I\cdot\vec{r}}|\beta'\rangle\langle\beta'|\vec{\epsilon}_F\cdot\vec{p}\,e^{-i\vec{k}_F\cdot\vec{r}}|\beta\rangle}{E_\alpha - E_{\beta'} - \hbar\omega_I}\right)\right].$$

Since we are interested in the quasi-elastic scattering, we choose the simple geometry $\vec{q}\,\|\,\vec{B}_0$ and select terms in $\gamma_{\alpha\beta}$ which have the form

$$\gamma_{\alpha\beta} = \gamma(k_{\beta z}, n_\beta, \sigma_\beta)\,\delta_{n_\alpha,n_\beta}\,\delta_{\sigma_\alpha,\sigma_\beta}\,\delta(k_{\beta y} - k_{\alpha y}) \times \delta(k_{\beta z} + q - k_{\alpha z})\,,$$

where the z direction is taken along $\vec{B}_0$. We define the scattering wave vector and frequency by $\vec{q} = \vec{k}_I - \vec{k}_F$ and $\omega = \omega_I - \omega_F$. Denoting the orbital relaxation time τ, the differential scattering cross section is given by[22]

$$\frac{d^2\sigma}{d\Omega d\omega} = \hbar\,\frac{\omega_F}{\omega_I}\,V\left(\frac{n_\omega+1}{\pi}\right)\mathrm{Im}\left\{\sum_\sigma\left(\frac{\omega}{\tilde{\omega}}\,L_2^{(1)}(\sigma) + \frac{1}{i\tilde{\omega}\tau}\,L_2^{(2)}(\sigma) - \frac{\omega}{\tilde{\omega}}\,\frac{[L_1^{(1)}(\sigma) - L_1^{(2)}(\sigma)][\tilde{L}_1^{(1)}(\sigma) - \tilde{L}_1^{(2)}(\sigma)]}{L_0^{(1)}(\sigma) + i\omega\tau L_0^{(2)}(\sigma)}\right) + \frac{v_q}{\epsilon}\left[\left(\sum_\sigma \frac{L_0^{(1)}(\sigma)L_1^{(2)}(\sigma) + i\omega\tau L_0^{(2)}(\sigma)L_1^{(1)}(\sigma)}{L_0^{(1)}(\sigma) + i\omega\tau L_0^{(2)}(\sigma)}\right)\left(\sum_\sigma \frac{L_0^{(1)}(\sigma)\tilde{L}_1^{(2)}(\sigma) + i\omega\tau L_0^{(2)}(\sigma)\tilde{L}_1^{(1)}(\sigma)}{L_0^{(1)}(\sigma) + i\omega\tau L_0^{(2)}(\sigma)}\right)\right]\right\}, \tag{1}$$

where

$$\tilde{\omega} = \omega - i/\tau, \quad v_q = 4\pi e^2/q^2, \quad n_\omega = (e^{\hbar\omega/kT} - 1)^{-1},$$

$$L_2^{(1,2)}(\sigma) = \frac{1}{V}\sum_{n,k_z,k_y} |\gamma(k_z, n, \sigma)|^2\,\Lambda^{(1,2)}_{k_z,k_z+q}\,, \tag{2}$$

$$L_1^{(1,2)}(\sigma) = \frac{1}{V}\sum_{n,k_z,k_y} \gamma^*(k_z, n, \sigma)\,\Lambda^{(1,2)}_{k_z,k_z+q}\,, \tag{3}$$

$$\tilde{L}_1^{(1,2)}(\sigma) = \frac{1}{V}\sum_{n,k_z,k_y} \gamma(k_z, n, \sigma)\,\Lambda^{(1,2)}_{k_z,k_z+q}\,, \tag{4}$$

$$L_0^{(1,2)}(\sigma) = \frac{1}{V}\sum_{n,k_z,k_y} \Lambda^{(1,2)}_{k_z,k_z+q}\,, \tag{5}$$

and ϵ is the longitudinal dielectric function

$$\epsilon(q, \omega) = \epsilon_\infty\,\frac{\omega_l^2 - \omega^2}{\omega_t^2 - \omega^2} - i\tilde{\omega}\tau v_q \sum_\sigma \frac{L_0^{(1)}(\sigma)L_0^{(2)}(\sigma)}{L_0^{(1)}(\sigma) + i\omega\tau L_0^{(2)}(\sigma)}\,. \tag{6}$$

In Eqs. (2)–(5) we have used the definitions

$$\Lambda^{(1)}_{k_z,k_z+q} = \frac{f(E(k_z, n, \sigma)) - f(E(k_z+q, n, \sigma))}{\hbar\tilde{\omega} + E(k_z, n, \sigma) - E(k_z+q, n, \sigma)} \tag{7}$$

and

$$\Lambda^{(2)}_{k_z,k_z+q} = \frac{f(E(k_z, n, \sigma)) - f(E(k_z+q, n, \sigma))}{E(k_z, n, \sigma) - E(k_z+q, n, \sigma)}\,. \tag{8}$$

The first term on the right-hand side of Eq. (6) is the sum of the electronic interband contributions to ϵ which give the optical dielectric constant ϵ_∞ and the optical-phonon contributions for polar semiconductors, where $\omega_l(\omega_t)$ is the zone-center, longitudinal- (transverse-) optical-phonon frequency. Note that Eqs. (1)–(8) are quite general and not restricted to spherical-band materials.

Although Eqs. (1)–(8) are rather complex in general, we can discern some interesting features of Eq. (1). Neglecting Coulomb interactions ($v_q = 0$), only the first summation in Eq. (1) contributes. For long relaxation times ($\omega\tau \gg 1$), this term reduces to

$$\frac{d^2\sigma}{d\Omega d\omega} = \hbar V \frac{\omega_F}{\omega_I} \frac{n_\omega + 1}{\pi} \frac{\mathrm{Im}}{V} \sum_{\substack{k_g, k_y \\ n, \sigma}} |\gamma(k_g, n, \sigma)|^2 \frac{f(E(k_g, n, \sigma)) - f(E(k_g + q, n, \sigma))}{\hbar(\omega - i/\tau) - \hbar^2 k_g q/m^* - \hbar^2 q^2/2m^*}, \tag{9}$$

which gives the cross section for scattering from unscreened single-particle excitations. The primary contributions to the cross section will be at frequencies along the branch cut(s) defined by $\omega = \hbar k_g q/m^* + \hbar q^2/2m^*$ (the zeros of the real part of the energy denominator). For a zero-temperature Fermi gas with $q \ll k_F$, there is one such distinct branch cut for each of the N occupied Landau levels, assuming that $\hbar\omega_c = O(E_F)$ so that the cuts are not overlapping. This leads to N distinct single-particle scattering peaks[15] centered at $\omega = q v_{Fn\sigma}$ where

$$v_{Fn\sigma} = [2/m^*]^{1/2}[E_F - (n + \tfrac{1}{2})\hbar\omega_c - \tfrac{1}{2}\sigma\hbar\omega_s]^{1/2}$$

is the velocity along $\vec{B}_0$ of an electron at the Fermi surface with orbital quantum number n and spin σ. In the absence of collisions $[(1/\tau) = 0]$, each peak has a width $\hbar q^2/m^*$. Each peak results from the scattering of a single particle on one Landau level from just inside to just outside the Fermi surface. The electrons on each occupied Landau level scatter the light independently, acting effectively as a one-dimensional electron gas.

Returning to Eq. (1), it can be shown that the inclusion of the Coulomb interaction terms leads to two important effects.[15,16] First, the single-particle scattering cross section is reduced, owing to screening of the charge-density fluctuations. Depending on the physical situation, this screening can be enormous[12,13] (see below). Second, for long relaxation times the scattering will have additional peaks, because of the excitation of LA plasma waves[17-19] at frequencies between the single-particle peaks. For a case in which there are N occupied Landau levels, there are $(N-1)$ possible acoustic modes. This rule applies only if all modes are well defined (not damped by single-particle excitations) and for $N \geq 2$. For one level occupied $(N = 1)$, no acoustic plasma waves can be excited[17-19] and the quasi-elastic scattering consists only of single-particle excitations. This results from the fact that the acoustic plasma wave involves, roughly, the motion of electrons on different levels in a manner yielding an almost charge-neutral wave.

The acoustic-plasma-wave scattering peaks occur at the frequencies given by $\mathrm{Re}(\epsilon) = 0$. This condition yields a maximum in $\mathrm{Im}(1/\epsilon)$. For long wavelengths $q \ll k_{Fn\sigma}$ [note that this condition fails for a level with $E(0, n, \sigma) \approx E_F$], one can show that

$$L_0^{(1)}(\sigma) \approx \frac{q}{2\hbar\pi^2\gamma_c^2} \sum_n \frac{q v_{Fn\sigma}}{\tilde{\omega}^2 - (q v_{Fn\sigma})^2} \tag{10}$$

and

$$L_0^{(2)}(\sigma) \approx -\frac{1}{2\hbar\pi^2\gamma_c^2} \sum_n \frac{1}{v_{Fn\sigma}}, \tag{11}$$

where $\gamma_c = \hbar/m^*\omega_c$. For the simple case in which only the two spin-split $n = 0$ levels are occupied, there is one acoustic wave and we find

$$\epsilon \approx \epsilon_\infty \left(\frac{\omega_t^2 - \omega^2}{\omega_t^2 - \tilde{\omega}^2}\right) - \frac{2}{\pi} \frac{e^2 q}{\hbar\omega} \left(\frac{1}{q^2\gamma_c^2}\right) Q, \tag{12}$$

where

$$Q = \frac{\tilde{\omega} q v_{F0+}}{\tilde{\omega}^2 - (q v_{F0+})^2(1 + 1/i\omega\tau)} + \frac{\tilde{\omega} q v_{F0-}}{\tilde{\omega}^2 - (q v_{F0-})^2(1 + 1/i\omega\tau)}. \tag{13}$$

Since for long wavelengths and low frequencies the coefficient in front of Q is large compared to ϵ_∞, the condition $\mathrm{Re}(\epsilon) = 0$ reduces approximately to $\mathrm{Re}(Q) = 0$. This feature is the essence of the acoustic plasma waves: Electrons on neighboring Landau levels give almost equal and opposite contributions to ϵ (and, therefore, almost equal and opposite density fluctuations) yielding a low-frequency plasma wave. Then for $\omega\tau \gg 1$ and ω near the acoustic-plasma-wave resonance, we calculate

$$\mathrm{Im}\left(\frac{1}{Q}\right) \approx -\frac{q^2 v_{F0+} v_{F0-}}{q(v_{F0+} + v_{F0-})\omega} \times \mathrm{Im}\left(\frac{q^2(v_{F0+} - v_{F0-})^2}{\omega(\omega - i/\tau) - q^2 v_{F0+} v_{F0-}}\right). \tag{14}$$

Thus, the acoustic-plasma-wave resonance occurs near $\omega = q(v_{F0+} v_{F0-})^{1/2}$ and has a full width $\approx 2/\tau$. Note that the condition for a weakly damped wave is $q(v_{F0+} v_{F0-})^{1/2}\tau \gg 1$, and that the wave velocity is the geometric mean of the two Fermi velocities.[16]

In Secs. III and IV, we will apply Eqs. (1)–(8) to specific model calculations of the quasi-elastic scattering spectra.

III. EFFECTIVE-MASS APPROXIMATION

In this section we consider a simple first approximation to light scattering in real semiconductors in which we use a one-band effective-mass Hamiltonian for coupling to the radiation field.[9,10] Such an approach can be valid only for $\hbar\omega_I$ small compared to any characteristic interband energies. The effect of the interband terms in γ is to produce an effective-mass correction so that $\gamma(k_g, n, \sigma)$

$= (e^2/mc^2)(m/m^*)\vec{\epsilon}_I \cdot \vec{\epsilon}_F$. Equation (1) then simplifies considerably, yielding[9,10]

$$\frac{d^2\sigma}{d\Omega d\omega} \approx \frac{\omega_F}{\omega_I}\left(\frac{n_\omega + 1}{\pi}\right)\sigma_T^*(\vec{\epsilon}_I \cdot \vec{\epsilon}_F)^2 \frac{\hbar V}{v_a} \times \epsilon_0^2(\omega)\,\mathrm{Im}\left(\frac{1}{\epsilon(\vec{q},\omega)}\right), \quad (15)$$

where $\sigma_T^* = (e^2/m^*c^2)^2$ is the effective Thomson cross section,

$$\epsilon_0(\omega) = \epsilon_\infty\left(\frac{\omega_l^2 - \omega^2}{\omega_t^2 - \omega^2}\right), \quad (16)$$

and ϵ is given by Eq. (6). The light effectively couples to longitudinal charge-density fluctuations and the scattering spectra show the peaks of $\mathrm{Im}(1/\epsilon)$. All scattering processes have the simple polarization selection rule $(\vec{\epsilon}_I \cdot \vec{\epsilon}_F)^2$. The nature of the quasi-elastic scattering spectra (see I) can be determined from the properties of the dielectric function.

Figure 1 shows the relative Stokes-scattering spectrum, computed using Eqs. (6) and (15) for zero-temperature n-type InSb with the following parameters, which will be used throughout the paper[23]: $m^*/m = 0.015$, $g^* = 50$, $\epsilon_\infty = 16$, $\omega_l/2\pi c = 193.8\ \mathrm{cm}^{-1}$, $\omega_t/2\pi c = 181.4\ \mathrm{cm}^{-1}$, and $n_e = 10^{17}\ \mathrm{cm}^{-3}$ for the carrier concentration. We have taken $\lambda_I = 10\ \mu$m, appropriate for experiments with a carbon-dioxide laser[6] and $\hbar\omega_c/E_F = 0.5$. These parameters yield $qv_F/2\pi c \approx 20\ \mathrm{cm}^{-1}$ for a right-angle scattering experiment. The dielectric function used

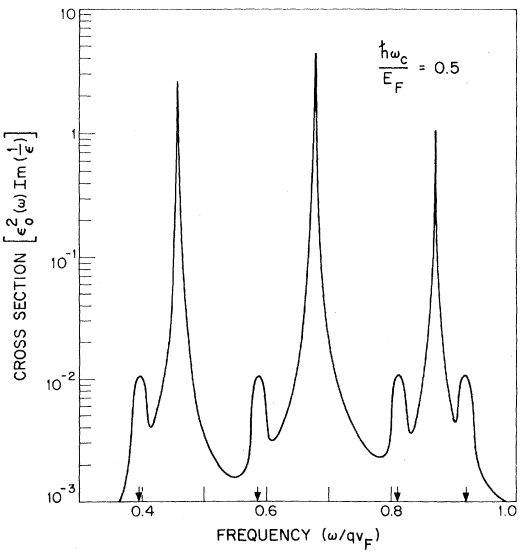

FIG. 1. Cross section vs frequency for InSb in the effective-mass approximation. The magnetic field is fixed; $qv_{F0}\tau = 500$, and $\lambda_I = 10\,\mu$m. The arrows denote the values of $\omega = qv_{Fn\sigma}$.

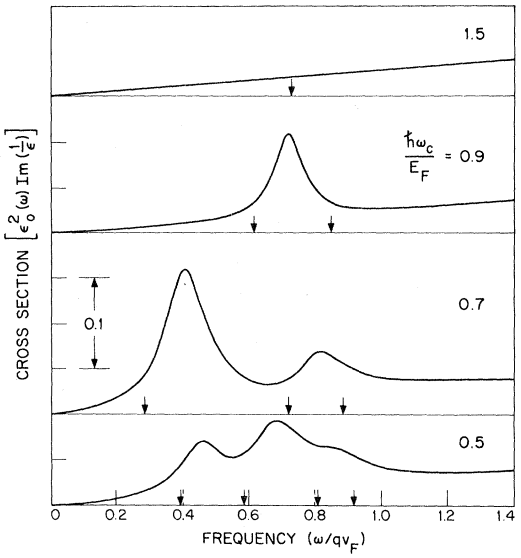

FIG. 2. Cross section vs frequency for InSb with magnetic field as a parameter. The effective-mass approximation is made, $qv_{F0}\tau = 10$, and $\lambda_I = 10\ \mu$m.

was computed numerically using exact closed-form expressions derived from Eq. (6). The curve was calculated for a very long relaxation time ($qv_{F0}\tau = 500$, where v_{F0} is the zero-field Fermi velocity) and illustrates the features described above. The three strong peaks each result from the excitation of an acoustic plasma wave and clearly dominate the scattering (note the logarithmic scale). The four small peaks result from single-electron excitations on each of the four occupied levels. Note the correlation of the latter peaks with the values of $qv_{Fn\sigma}$, which are marked by the arrows. For somewhat shorter relaxation times the single-particle peaks will be completely obscured by the dominant acoustic-plasma-wave scattering.

Figure 2 shows the development of the spectra as the magnetic field is varied for a $(qv_{F0}\tau) = 10$. Each curve in Fig. 2 is computed with the correct $(qv_F\tau)$ which differs slightly from 10, owing to the variation of the Fermi energy with magnetic field. Each bump in the lower curves results from a peak in the acoustic wave scattering which is completely dominant, as expected. As the magnetic field increases there are fewer and fewer levels occupied and, therefore, fewer scattering peaks. For $\hbar\omega_c/E_F = 1.5$, there is only one Landau level occupied and no acoustic waves can be excited. At first sight, the monotonic rise in the scattering with no peak at qv_{F0+} for this case is rather curious. However, following this curve out to the region of the (optical) plasmon peak ($\omega \approx \omega_p$) shows that the behavior of the low-frequency scattering is dominated by the wing (or tail) of the plasmon scattering. The single-particle excitation peak is completely lost for this

short value of τ.

Although this model calculation illustrates some of the general features of magnetoplasma quasi-elastic scattering, it is not expected to be quantitatively accurate of InSb. A value of $qv_{F0}\tau = 10$ is optimistic by a factor of 5 for 10-μm light and n-InSb with $n_e \approx 10^{17}$ cm^{-3} and $T \approx 0$. For $qv_{F0}\tau = 2$ ($\tau \approx 5\times10^{-13}$ sec), the peaked spectra of Fig. 2 are strongly smeared and tend to become lost in the wings of the plasmon scattering, as is the case for the top curve. Also, the effective-mass approximation neglects coupling mechanisms involving the spin degree of freedom and spin-orbit coupling which are important in real semiconductors.[13,15,16,24-26] These mechanisms can significantly alter the order of magnitude of the cross section, the polarization selection rules, and the nature of the line shapes. A more realistic calculation is given in Sec. IV.

IV. III-V COMPOUNDS: INDIUM ANTIMONIDE

The first problem one faces in treating complex semiconductors such as the III-V compounds is the proper calculation of $\gamma_{\alpha\beta}$. Several papers[24-26] have been written on the evaluation of the interband matrix elements in $\gamma_{\alpha\beta}$ for specific scattering processes such as inter-Landau-level scattering. Some useful approximations for reducing γ are given in I. We will make the dipole approximation[24,26] ($e^{i\vec{k}_I\cdot\vec{r}}, e^{-i\vec{k}_F\cdot\vec{r}} \approx 1$) and consider only interband intermediate-state contributions to γ since these are the largest. We neglect intermediate states other than the three P-like valence bands since their contributions should be small.[27] Since the direct gaps for these three bands E_{gi} are large compared to typical $\hbar\omega_c$, E_F, and ω, we replace the denominators in the expression for $\gamma_{\alpha\beta}$ by $E_{gi} \pm \hbar\omega_I$. This procedure is reasonable as long as $(E_{gi} - \hbar\omega_I) \gg \hbar\omega$. To make things tractable we adopt a decoupled band scheme,[26] assuming the conduction band is pure S like, the split-off band is pure P like, $|\frac{1}{2}, \pm\frac{1}{2}\rangle$, and only the light and heavy holes are mixed by a finite k_z. This scheme picks out the major character of the wave functions for the four bands, thus giving the most important terms in γ. Finally, we make the band-edge approximation ($k_z = 0$) in evaluating the matrix elements of p. This last approximation is less appropriate than the others. It is made largely for simplicity and has important consequences which will be discussed below. We find

$$\gamma(0, n, \sigma) \approx (e^2/mc^2)\,[A\,\vec{\epsilon}_I\cdot\vec{\epsilon}_F + i\sigma B\,(\vec{\epsilon}_I\times\vec{\epsilon}_F)_z]\,, \tag{17}$$

where

$$A = 1 + \frac{2P^2}{3m}\left(\frac{E_g}{E_g^2 - (\hbar\omega_I)^2} + \frac{E_g + \Delta}{(E_g+\Delta)^2 - (\hbar\omega_I)^2}\right) \tag{18}$$

and

$$B = \hbar\omega_I \frac{2P^2}{3m}\left(\frac{1}{E_g^2 - (\hbar\omega_I)^2} - \frac{1}{(E_g+\Delta)^2 - (\hbar\omega_I)^2}\right)\,. \tag{19}$$

In Eqs. (18) and (19), E_g is the direct-energy band gap of InSb, Δ is the valence-band spin-orbit splitting, and $P = -i\langle S|\, p_z|\, Z\rangle$ is the interband momentum matrix element. Note that in the limit $\hbar\omega_I \ll E_g$, $A \approx m/m^*$, and $B \approx 0$. Note also that B goes to zero as the spin-orbit parameter (Δ/E_g) goes to zero. The results embodied in Eqs. (17)–(19) are rather surprising since $\gamma(0, n, \sigma)$ is independent of the Landau-level quantum number. Equation (17) is, in fact, identical to one component of the zero-field result for γ found by Hamilton and McWhorter.[13] Each of the individual contributions to γ does depend on n, but the sum is independent of $\underline{n}$. While this result is appealing because of its simplicity, it is peculiar to our approximate calculation and we will find that it leads to overestimation of screening effects. In general, both A and B depend on $\underline{n}$ and k_z.

The simple form for γ [Eq. (17)] leads to simplification of the cross-section expression Eq. (1):

$$\frac{d^2\sigma}{d\Omega d\omega} \approx \sigma_T \frac{\hbar V}{\pi v_q}\,[A^2(\vec{\epsilon}_I\cdot\vec{\epsilon}_F)^2\epsilon_0^2(\omega)\,\mathrm{Im}(1/\epsilon) + B^2\,(\vec{\epsilon}_I\times\vec{\epsilon}_F)_z^2\,\mathrm{Im}(J)]\,, \tag{20}$$

where

$$J = -\epsilon - \tilde{\omega}^2\tau^2\frac{v_q^2}{\epsilon}\left(\sum_\sigma \frac{\sigma L_0^{(1)}(\sigma)\,L_0^{(2)}(\sigma)}{L_0^{(1)}(\sigma) + i\omega\tau L_0^{(2)}(\sigma)}\right)^2\,, \tag{21}$$

and we have assumed $\omega_F \approx \omega_I$ and zero temperature. For the form of γ given by Eq. (17), the two components of γ give independent noninterfering contributions to the cross section proportional to A^2 and B^2, respectively. The first term ($\propto A^2$) results from coupling to charge-density fluctuations, while the second term ($\propto B^2$) results from coupling to spin-density fluctuations[13,16] via virtual interband transitions. Only the second term was considered by Wolff[16] in his discussion of the acoustic-plasma-wave scattering. Wolff's results are obtained from Eq. (20) if one sets A and $1/\tau$ equal to zero.

Equations (20) and (21) do not correctly treat inter-Landau-level (including spin-flip) processes.[24-26,28] The following discussion and computations assume that the magnetic field is strong enough to remove these scattering peaks from the quasi-elastic regime ($\omega_c,\ \omega_s > qv_F$). Plasmon scattering is correctly included in the expressions.

In the limit $\hbar\omega_I/E_g \to 0$, we are left with only the first term on the right-hand side of Eq. (20), and the result is identical with the effective-mass re-

sult Eq. (15). Therefore, within the approximations made above, the scattering spectra with the polarization rule $(\vec{\epsilon}_I \cdot \vec{\epsilon}_F)^2$ have the behavior computed in Sec. III. The results merely need to be scaled by a constant factor. It should be noted that this result is peculiar to the simple form used for γ in which A is independent of the orbital quantum numbers. This approximation gives a cross section $\propto \mathrm{Im}(1/\epsilon)$ which predicts very heavy screening of the quasi-elastic excitations as discussed in Sec. III. If one uses a correct expression for A which includes its dependence on orbital quantum numbers, the cross-section expression is much more complex than $\mathrm{Im}(1/\epsilon)$ and the cross section can be orders of magnitude larger as a result of the reduction in screening. The actual results one obtains are very sensitive to the form of A since the result $\mathrm{Im}(1/\epsilon)$ gives a small number resulting from the cancellation of two large numbers. This phenomena is analogous to the strong reduction in screening of zero-field quasi-elastic scattering.[12,13]

In an actual experiment one can distinguish the two contributions to the cross section in Eq. (20) by appropriately arranging the scattering geometry and analyzing the scattered light. Therefore, we present in this section a separate calculation of the scattering spectra given by the second contribution $[\propto(\vec{\epsilon}_I \times \vec{\epsilon}_F)_z^2]$. First, note that in the extreme quantum limit where B_0 is so large that only one Landau level is occupied, one has

$$\mathrm{Im}(J) = \epsilon_0^2(\omega)\,\mathrm{Im}(1/\epsilon)\ . \tag{22}$$

Again, the scattering spectra have the form given in Sec. III and the screening of the single-particle excitations will be grossly overestimated. A set of quasi-elastic scattering spectra $[\mathrm{Im}(J)]$ for n-type InSb are shown in Fig. 3. The parameters

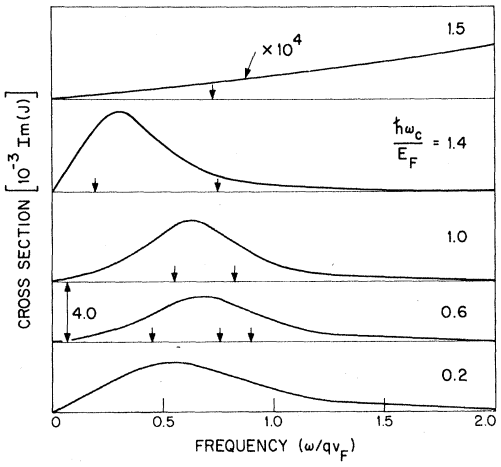

FIG. 3. Quasi-elastic scattering spectra for InSb with magnetic field as a parameter. The theory of Sec. IV is used, $qv_{F0}\tau = 2$, and $\lambda_I = 10$ μm.

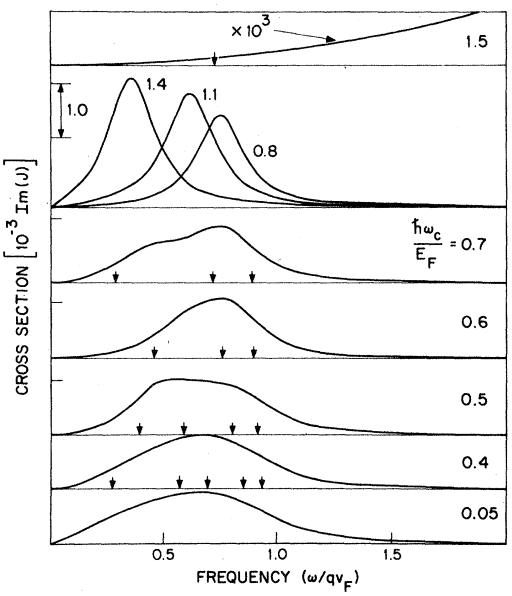

FIG. 4. Scattering spectra for InSb with magnetic field as a parameter $[(qv_{F0}\tau) = 4,\ \lambda_I = 5\,\mu\mathrm{m}]$. For $\hbar\omega_c/E_F = 0.8$, 1.1, 1.4 there are only two levels occupied.

chosen were the same as those of Sec. III with the exception of the choice $(qv_{F0}\tau) = 2.0$, which is realistic for $\lambda_I = 10$ μm and $n_e = 10^{17}$ cm^{-3} in InSb. There are several important characteristics of the curves of Fig. 3. First, the relative cross-section scale in Fig. 3 is *four orders of magnitude larger* than the scale for Fig. 2. This results because of ineffective screening of the spin-density fluctuations associated with the B driving term in γ. [Mathematically, the second term on the right-hand side of Eq. (21) subtracts very little from the first term. However, for $\hbar\omega_c/E_F = 1.5$ there is only one level occupied, so that Eq. (22) applies, and a spin-density perturbation inherently involves a charge-density perturbation which is heavily screened. The scattering in the quasi-elastic regime drops by orders of magnitude. As stated above, this latter result is an artificial feature of the theoretical model. While one expects the high-field screening to be larger, the actual reduction will depend critically on the behavior of $B(n, k_z)$. Finally, note that even for the realistic value of τ chosen, the spectra of Fig. 3 are not dominated by the wing of the plasmon peak due to ineffective screening of the spin-density oscillations.

As an additional example, Fig. 4 gives a set of spectra for $\lambda_I = 5.0$ μm and $(qv_{F0}\tau) = 4.0$. Such conditions are roughly appropriate for experiments using a carbon-monoxide gas laser.[7] This case is interesting because the cross-section enhancement obtained by using a 5-μ light source would improve the chances of observation. For the cases in which

only two levels are occupied ($\hbar\omega_c/E_F = 0.8, 1.1, 1.4$) the spectra have a sharp well-defined peak due to acoustic-plasma-wave scattering. For the conditions of both Figs. 3 and 4, the dominant contribution to the spectra at weak fields is from $\mathrm{Im}(\epsilon)$, which is the first term in $\mathrm{Im}(J)$. This implies that electron-electron interactions can be ignored in computing the cross section. Also, since the collective-mode scattering derives from the second term in J [Eq. (21)], the scattering is predominantly single-particle excitations. Both of these features are consistent with the zero-field calculations of Hamilton and McWhorter.[13] At higher fields (two levels occupied) the second term on the right-hand side of Eq. (21) predominates, yielding acoustic-plasma-wave scattering. At still higher fields ($\hbar\omega_c/E_F = 1.5$, one level occupied) the two terms give almost equal and opposite contributions to $\mathrm{Im}(J)$ and the cross section is dramatically reduced.

Finally, it is of interest to examine the behavior of this depolarized (B-term) scattering in the vicinity of plasma resonance. A set of spectra with magnetic field as a parameter is shown in Fig. 5. The physical parameters are the same as those of Fig. 4. There are two peaks in the high-field spectra which result from excitation of coupled plasmon-phonon modes.[3-7] These peaks disappear at low fields. This result is important for the interpretation of experimental results since it indicates the presence of an additional mechanism, besides electrooptic coupling,[4,11] for the occurrence of depolarized plasmon scattering. Physically, this scattering has its origin in the fact that the spin-density driving term inherently induces charge-density fluctuations in the electron plasma in a strong magnetic field. These charge-density fluctuations are driven resonantly at the plasma frequency, yielding the plasmon-scattering peak. This phenomenon is most easily visualized for the case in which all the electrons are in the lowest

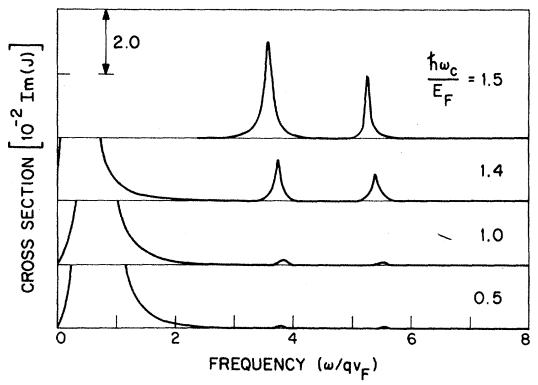

FIG. 5. B-term plasmon scattering spectra for InSb with magnetic field as a parameter [$(qv_{F0}\tau) = 4$, $\lambda_I = 5\,\mu$m].

(0, +) Landau level, having all their spins aligned.

It should be emphasized that Eqs. (17)–(19) are not quantitatively accurate under strong resonance enhancement which would occur for experiments with sources in the 5–6-μm range with InSb. The full and correct energy denominators in $\gamma_{\alpha\beta}$ must be kept, in order to obtain accurate scattering efficiencies. However, the qualitative nature of the spectra of Figs. 4 and 5 will not be affected by such details.

V. DISCUSSION

One of the most striking features of the results given above is the very large difference in the magnitudes of screened and unscreened quasi-elastic scatterings. Any scattering processes for which $\gamma(n, k_z, \sigma)$ is constant occurs entirely through coupling to charge-density excitations and is heavily screened in the quasi-elastic regime (for long wavelengths). Because of the form of the cross-section expressions, the theoretical scattering spectra are very sensitive, both in magnitude and shape, to the specific form of γ used. Similar difficulties were encountered in discussions of zero-field spectra.[13] Since we know in general that A will be dependent on the orbital quantum numbers, the features of the A-term scattering [$\propto (\vec{\epsilon}_I \cdot \vec{\epsilon}_F)^2$], which are given qualitatively by the discussion of Sec. III, are misleading. We expect the size of this scattering to be much larger than that indicated by Figs. 1 and 2. This may also remove the difficulty of the quasi-elastic spectra being lost in the wing of the plasmon scattering. A theory which is accurate on this point requires a full (and very complex) calculation of γ without making the approximations of Sec. IV. Such a computation is probably warranted only for a detailed comparison with experimental data. The same difficulty is encountered for the B-term scattering in the high field (one level occupied) where the cross section reduces to the form $\mathrm{Im}(1/\epsilon)$. While the single-particle spectrum is likely to be weak in this case, the reduction will not be nearly so large as that indicated.

The physical parameters chosen for the calculations of Secs. III and IV are not to be viewed as particularly restricted. They were chosen to be in a range thought to be accessible by experimental observation.[6,7] Most of the parameters can be changed significantly without changing any of the qualitative features of the results. The only exception is that all the above discussion applies to the long-wavelength case $q \ll k_F$, k_{sc}, where k_{sc} is a characteristic screening wave vector. Reversing the latter inequality to $q \gg k_{sc}$ will greatly alter the screening effects.

It is of interest to estimate the actual scattering efficiencies expected for the quasi-elastic scatter-

ing. We define the total scattering efficiency as $S = (1/V)(d\sigma/d\Omega)$, where $(d\sigma/d\Omega)$ is the differential cross section integrated over the spectrum (or line) in question. For $m^*/m = 0.015$, $\sigma_T^* = 3.5 \times 10^{-22}$ cm^2. For right-angle scattering ($\vec{k}_I \perp \vec{k}_F$), $\epsilon_\infty = 16$, and $\lambda_I = 10$ μm, we estimate $S_B \approx 10^{-8}$ sr^{-1} cm^{-1} for the B-term scattering. This scattering efficiency is roughly that estimated for the A-term plasmon scattering which has been observed in zero-field 5-μ experiments.[7] We estimate $S_A = 10^{-11}$ sr^{-1} cm^{-1}, but this number is not expected to be reliable because of the overestimation of the screening. Estimates of scattering efficiencies for 5-μ experiments have not been made, owing to the uncertainty in the enhancement factors under conditions of strong resonant enhancement. The efficiencies will certainly be larger than those quoted for 10-μ experiments.

The size of the estimated scattering efficiencies, coupled with the well-defined line shape of the scattering from the acoustic plasma wave in high magnetic fields, yields a favorable prognosis for the actual observation of the acoustic plasma wave in infrared experiments with InSb. For 5-μ experiments, $(qv_F/2\pi c) \approx 40$ cm^{-1} for $n_e = 10^{17}$ cm^{-3}, and the acoustic-plasma-wave linewidth at high fields ($\gtrsim 70$ kG) is about 10–15 cm^{-1}. Such a line should be observable. It would be most interesting to measure the scattering spectra at still higher fields (~ 100 kG) where only one level is occupied. The behavior of these spectra and the A-term (diagonal) scattering will tell how much the strong screening is obviated by the complex energy bands of InSb.

ACKNOWLEDGMENT

We are grateful to A. L. McWhorter for interesting and helpful discussions.

*Work sponsored by the Department of the Air Force.

[1]D. Pines, *Elementary Excitations in Solids* (Benjamin, New York, 1964), Chap. 4.

[2]For simplicity, we ignore phonon effects and assume $\omega_p > qv_c$ in this discussion.

[3]A. Mooradian and G. B. Wright, Phys. Rev. Letters 16, 999 (1966).

[4]A. Mooradian and A. L. McWhorter, Phys. Rev. Letters 19, 849 (1967); A. Mooradian and A. L. McWhorter, in *Light Scattering Spectra of Solids*, edited by G. B. Wright (Springer-Verlag, New York, 1969), p. 297.

[5]B. Tell and R. J. Martin, Phys. Rev. 167, 381 (1968).

[6]C. K. N. Patel and R. E. Slusher, Phys. Rev. 167, 413 (1968).

[7]F. A. Blum and A. Mooradian, in *Proceedings of the Tenth International Conference on Semiconductors*, edited by S. P. Keller, J. C. Hensel, and F. Stern (U. S. Atomic Energy Commission, Oak Ridge, Tenn., 1970), p.755.

[8]A. Mooradian, Phys. Rev. Letters 20, 1102 (1968); in *Light Scattering Spectra of Solids*, edited by G. B. Wright (Springer-Verlag, New York, 1969), p. 285.

[9]A. L. McWhorter, in *Proceedings of the International Conference on Quantum Electronics, Puerto Rico*, 1965 (McGraw-Hill, New York, 1965), p. 111.

[10]P. M. Platzman, Phys. Rev. 139, A379 (1965).

[11]E. Burstein, A. Pinczuk, and S. Iwasa, Phys. Rev. 157, 611 (1967).

[12]P. A. Wolff, Phys. Rev. 171, 436 (1968); in *Light Scattering Spectra of Solids*, edited by G. B. Wright (Springer-Verlag, New York, 1969), p. 273.

[13]D. C. Hamilton and A. L. McWhorter, in *Light Scattering Spectra of Solids*, edited by G. B. Wright (Springer-Verlag, New York, 1969), p. 309.

[14]S. S. Jha, Phys. Rev. 179, 764 (1969); 182, 815 (1969).

[15]F. A. Blum, Phys. Rev. B 1, 1125 (1970). This paper will be referred to as I in the text.

[16]P. A. Wolff, Phys. Rev. B 1, 164 (1970).

[17]A. L. McWhorter and W. G. May, IBM J. Res. Develop. 8, 285 (1965).

[18]S. L. Ginzburg, O. V. Konstantinov, and V. I. Perel, Fiz. Tverd. Tela 9, 2139 (1967) [Sov. Phys. Solid State 9, 1684 (1968)]; O. V. Konstantinov and V. I. Perel, Zh. Eksperim. i Teor. Fiz. 53, 2034 (1967) [Sov. Phys. JETP 26, 1151 (1961)].

[19]G. Benford and D. Book, Phys. Rev. Letters 21, 808 (1968).

[20]D. Pines, Can. J. Phys. 34, 1379 (1956).

[21]D. Pines and J. R. Schrieffer, Phys. Rev. 124, 1387 (1961).

[22]R. W. Davies and F. A. Blum, Phys. Rev. B 3, 3321 (1971).

[23]The conduction band of InSb is rather nonparabolic. Since the precise values of m^* and g^* are unimportant for the problem at hand, the values used are chosen to be representative. See, for example, E. J. Johnson and D. H. Dickey, Phys. Rev. B 1, 2676 (1970). Our calculations are also rather insensitive to the values of ω_l and ω_t used. The values quoted are from Raman-scattering data: K. W. Nill and A. Mooradian, Bull. Am. Phys. Soc. 13, 1658 (1968); (unpublished).

[24]Y. Yafet, Phys. Rev. 152, 858 (1966).

[25]V. P. Makarov, Zh. Eksperim. i Teor. Fiz. 55, 704 (1968) [Sov. Phys. JETP 28, 366 (1969)].

[26]G. B. Wright, P. L. Kelley, and S. H. Groves, in *Light Scattering Spectra of Solids*, edited by G. B. Wright (Springer-Verlag, New York, 1969), p. 335.

[27]There are several relevant discussions of the band structure of InSb in a magnetic field in the literature: Y. Yafet, Phys. Rev. 115, 1172 (1959); C. R. Pidgeon and R. N. Brown, *ibid.* 146, 575 (1966).

[28]R. E. Slusher, C. K. N. Patel, and P. A. Fleury, Phys. Rev. Letters 18, 77 (1967); C. K. N. Patel and E. D. Shaw, *ibid.* 24, 451 (1970).